Journal of Advanced Research in Applied Sciences and Engineering Technology

Journal homepage:
https://semarakilmu.com.my/journals/index.php/applied_sciences_eng_tech/index
ISSN: 2462-1943


# Analysis and Modeling of Surface Roughness in Powder Mix EDM and Pure EDM Using Central Composite Design

Zakaria Mohd Zain[1], Mir Akmam Noor Rashid[1,*], Sher Afghan Khan[2], Ahsan Ali Khan[1]

[1] Department of Manufacturing & Materials Engineering, International Islamic University Malaysia, Gombak, 53100 Selangor, Malaysia
[2] Department of Mechanical Engineering, International Islamic University Malaysia, Gombak, 53100 Selangor, Malaysia

**ARTICLE INFO**

***Article history:***
Received 16 December 2022
Received in revised form 17 February 2023
Accepted 26 February 2023
Available online 18 March 2023

***Keywords:***
Surface modification; Tantalum Carbide powder; EDM; central composite design

**ABSTRACT**

Conventional surface modification methods, such as ion insertion and laser surface melting, have recently seen growing importance in the innovative usage of the electrical discharge machining process (EDM) as a competitive substitute. Surface composition and properties are affected by several factors, including erosion of work materials and tool materials during the process, as well as the formation of plasma channels from the vaporized materials. This indicates that, under certain machining conditions, deliberate materials transfer may be possible using either a composite electrode by scattering metallic powders in a dielectric or a combination of the two. However, the traditional electrode has not been very successful in the surface modification process. Although it has been considered, expanding research into the use of powder additives through EDM techniques to enhance the level of surface modification is lacking. In addition, the pulse interval is not included in the existing works that examine the impact of technique parameters on surface modification. Because of this, a thorough optimization of the process has not been possible to characterize the connection between the independent variables under control and the machining parameters. To take full advantage of the benefits offered by EDM, it is necessary to learn more about the missing links between the process and its desired outcomes, such as whether or not surface alloying of metallic materials using EDM is feasible and what controls should be used for the various variables involved. The purpose of this study was to assess the efficiency of EDM-based surface alloying of stainless steel using Tantalum Carbide (TaC) powder as an additive by measuring the resulting surfaces' roughness (SR). It was found that $Ra_{PMEDM}$ 11 μm recorded at current 5A and on-time 6.30 μs, off-time 7.00 μswith powder concentration 25g/L. The $Ra_{PMEDM}$ is easy to predict by controlling factor current (A) and on-time (B). At the higher current of 7.25A, $Ra_{PMEDM}$ showed to decrease slightly. This result justifies TaC powder starts to control and modify the surface of stainless steel at a high factor current. In the case of without additives RaEDM, at maximum current 5 A, on-time 6.26 μs, and off-time 7 μs, RaEDM recorded 7 μm. Although it provided the highest Ra compared to $Ra_{PMEDM}$.

[*] *Corresponding author.*
*E-mail address: noorakmam@gmail.com*

https://doi.org/10.37934/araset.30.1.243254

## 1. Introduction

The tool and die industry makes extensive use of EDM, making it one of the best prevalent non-traditional machining methods. Strong, hard, or intricately shaped materials are ideal candidates for this treatment [1]. In recent years, additive manufacturing has established itself as a go-to for making prototypes and low-volume production parts. Due to the tool's lack of contact with the workpiece, even thin sections and brittle materials can be machined without deformation [2].

The electrical discharge machining (EDM) procedure has seen a renaissance in popularity over the past few decades, thanks in large part to the attention it has garnered for its potential in surface modification of various material plasma channels formed by material vapors from eroding work material and tool electrode, pyrolysis of dielectric, erosion of work material during process, and removal of some tool materials affect the surface composition and properties. Using composite electrodes or dispersing metallic powders in the dielectric, or both may allow deliberate material transfer under certain machining conditions [3].

Electrical discharge machining (EDM) is used for hard or non-machinable metals [4,15]. Electrical discharge machining (EDM) removes material from a part using a series of electrical discharges. EDM separates the tool and workpiece with a dielectric fluid medium and applies discrete discharges. Spark discharges melt and evaporate a minor amount of workpiece material across a gap (spark gap) between the tool and the workpiece [5]. During a machining process, spark discharges always happen at the highest electrical potential point, which floats around the machining gap at random [6,16]. Steel with extremely high hardness and unusual metals such as Inconel, Hastelloy, Kovar, titanium, tungsten, silicon, nickel, cobalt, carbide, and so on. is routinely machined with great precision using EDM [6]. The EDM cutting tool is positioned so that it comes within millimeters of the work without actually cutting into it. Fast, successive sparks melt and vaporize material along the cutting path, leaving a series of tiny craters in the workpiece. The particles are washed away by the constantly flowing dielectric fluid. While traditionally used in the mold-making tools and dies industries, especially in the aerospace and electronics sectors, EDM machining is rapidly becoming a go-to technique for fabricating production and prototype parts across many sectors [7].

Rapid advancements have made EDM an indispensable tool for die and mold machining, micro-machining, and prototyping. The EDM process known as "EDM die-sinking" is one of the most popular EDM operations. Plastic injection and other mold fabrication processes are far more common than die-sinking applications. New applications for flourishing industries like the aerospace sector have contributed to the ongoing use and expansion of the EDM process' capabilities [8]. Success has been found in using EDMs to machine tough materials that are difficult for conventional machining methods to work with. Titanium and nickel-based alloys are two examples of materials with low thermal conductivity and high strength, which causes difficulties in mechanical cutting processes and makes it difficult to produce a high-quality end product. However, EDM technology allows for the efficient and effective machining of these materials, leading to a rise in the use of EDMs in the aerospace industries [9]. Metals, metal alloys, compounds, graphite, and even some ceramic materials of varying hardnesses are all commonly machined using EDM in a variety of industrial settings [10]. This study assessed the effectiveness of TaC compacted powder using surface roughness (SR), tool wear rate (TWR), micro harness (Hv), material removal rate (MRR), percentage material migration, and corrosion resistance. Mathematical models have been developed, and the EDM process has been optimized, to explain the relationship between the machining parameters and the independent variables (like the amount of TaC powder in the dielectric) (i.e. input current, Ip, and on-off time). The findings of this research are anticipated to aid in identifying the optimal EDM settings for surface-modifying stainless steel, as well as identifying the relevant independent controllable factors. Additionally, also explored the feasibility of using an EDM machine for surface modification/alloying of stainless steel.

## 2. Materials and Methodology

### *2.1 Workpiece: Stainless Steel*

Stainless steel is well known because of its corrosion and oxidation resistance due to the chromium-rich oxide layer on the surface layer of alloyed steel. Besides that, it is also tougher and has higher ductility besides having higher hot strength which means, it can operate at high temperatures and retain its strength. Figure 1 shows the stainless steel workpiece used in the experiment and the EDM machine used for the experiment. Copper was utilized as the electrode material and tool in this study. Copper's high thermal and electrical conductivity make it a desirable material. It is an excellent thermal conductor, electrical conductor, building material, and alloying component [11].


(a) (b)

**Fig. 1.** (a) The stainless steel workpiece and (b) the EDM machine

Figure 2 illustrates the copper workpiece used in the experiment and the properties of copper is summarized in Table 1. It has a dimension of 50mm x 30mm x 10mm. As we required a parallel and less distorted contact surface of 10mm x 10mm, the electrode was cut by wire EDM. They were also ground to ensure that the adjacent surfaces are parallel. A total of 6 electrodes are prepared.

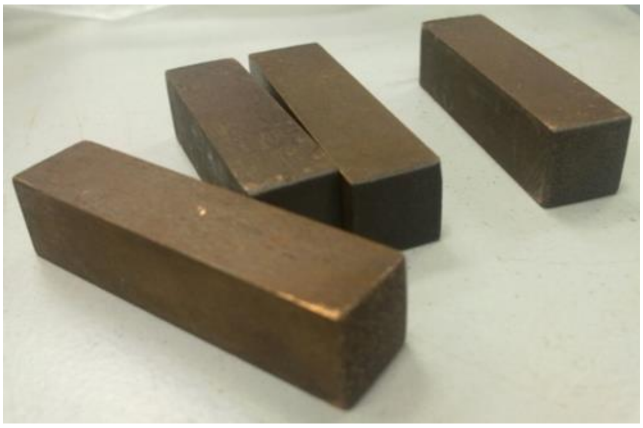

**Fig. 2.** Copper workpiece

### *2.2 Powder: Tantalum Carbide (TaC)*

Extremely hard, with a Mohs scale hardness of 9–10, as stated by Uhlmann and Roehner [11]. Only diamond is harder than this material. It is an important cermet material and weighs a lot as a dark to light brown powder that is processed by sintering. It is sometimes added to tungsten carbide alloys as a fine-crystalline additive.

It is status of the stoichiometric binary compound with the highest measured melting point of 3880 °C. The melting point of the sub-stoichiometric compound TaC is higher, hovering around 4000 degrees Celsius. As a result, it produces a spectacular flash when exposed to air and is only marginally soluble in acids.

### *2.3 Dielectric Fluid*

Kerosene is commonly utilized as a dielectric fluid in die-sinking EDM due to the benefits it provides in terms of decreased tool wear, improved precision, and enhanced surface quality [12]. The corroded particles between the workpiece and the electrode can be cooled by passing a current through a dielectric fluid, which also acts as a dielectric barrier for the spark. Due to these qualities, kerosene has been selected as the dielectric fluid to be used in the experiments.

### *2.4 Design of Experiment (DOE)*

The analysis of experimental data, as opposed to theoretical models, is at the heart of experimental design, which is a strategy for acquiring empirical knowledge. It can be used whenever more information is needed about a phenomenon, or when existing information needs to be upgraded. The first steps in designing an experiment are to establish its goals and to decide on the process variables and study outcomes.

In this investigation, we employ the factorial design and RSM of the DOE (RSM). Empirical modeling with polynomials as local approximations to achieve accurate input/output relationships is achieved with the RSM [13].

### *2.5 Process Parameters*

In any DOE, determining the process parameter is the key. Table 1 discloses the process parameters that have been used for the experimentation. From Table 1, it can be seen that there are four factors which are concentrations, peak current, on-time, and off-time. Table 2 shows the 5 levels of input parameters.

**Table 1**
The parameters and level values were selected for the experiments

| Parameter/Factors | Low value | High value |
|---|---|---|
| Concentration (TaC), $C_t$ | 5g/L | 45g/L |
| Peak Current, $I_p$ | 2A | 8A |
| On-Time, $T_{on}$ | 5.5µs | 7.1µs |
| Off-Time, $T_{off}$ | 6.0 µs | 8.0µs |

**Table 2**
Values of machining variable and levels

| Variables | -2 | -1 | 0 | 1 | 2 |
|---|---|---|---|---|---|
| Concentration (TaC), $C_t$ | 5 | 15 | 25 | 35 | 45 |
| Peak Current, $I_p$ | 2 | 3.5 | 5 | 6.5 | 8 |
| On-Time, $T_{on}$ | 5.5 | 5.9 | 6.3 | 6.7 | 7.1 |
| Off-Time, $T_{off}$ | 6 | 6.5 | 7 | 7.5 | 8 |

### *2.6 Surface Roughness*

As far as surface roughness is concerned, there are several ways used to indicate the degree of roughness of a surface. One method which is widely used is the Center Line Average Method ($R_a$). $R_a$ is the average roughness value of the profile that depicts the profile points' average absolute deviation from a mean line. Mitutoyo Surftest (Figure 3) was used to measure surface roughness (Ra) (SV-514). Software called Surfpak V4.10 (2) is being employed.

**Fig. 3.** Mitutoyo Surftester

### *2.7 Machine Setup*

A Mitsubishi EX22 die-sinking EDM machine is employed in the experiment. Jet flushing was adequate for our experiment. The setup that was used in all the experiments is shown in Figure 4(a) and Figure 4(b) represent the photo of the Mitsubishi EX22 die-sinking EDM machine and the physical setup of the EDM machine. The following section comprises the setup procedure (preparation of experimentation) of the EDM machine.


(a) (b)

**Fig. 4.** (a) MITSUBISHI EX22 die-sinking EDM, (b) Experimental setup for Die Sinking EDM

Firstly, the experimental operation is prepared as shown in Figure 4. To limit the excess use of powder and as well as dielectric fluid (kerosene), instead of using the whole tank, a comparatively smaller (250 × 250× 100 mm) container is used where the machining takes place. To avoid sedimentation of powder particles at the bottom, a stirring system is provided in terms of air flushing. Then, both the workpiece and tool are weighed using a single pan electric balance and their weights are recorded. A corresponding weight of TaC powder is measured using the same electric balance to get the required concentration. Next, the workpiece is a fixture within the container where a suitable concentration of powder-mixed kerosene dielectric has been added based on the DOE. Meanwhile, the tool is mounted on the tool holder of the Mitsubishi EX22 die-sinking EDM machine. The input parameters are entered and the EDM process started. After each experiment/run the machining time is recorded. After each experiment/run is complete, both the workpiece and tool are weighed. The difference in weight is used to calculate MRR and TWR.

### *2.8 Experimental and Measurement Procedures*

In this section, the procedures to measure the output parameter of Surface roughness (Ra) will be explained. Mitutoyo Surftest (SV-514) was used to determine the surface roughness (Ra) parameters in this research. The tester applies Surfpak V4.10 (2) software with a resolution of 0.01µm and a stylus speed of 0.10mm/s. The tester uses a low-pass filter with 50% amplitude transmittance at the cut-off length. Mitutoyo Surftest (Figure 3) is a contact-type profile meter that amplifies the vertical motion of a stylus as it is drawn across the surface. Concerning the equipment's operating manual, the recommended values for machining operation whose average mean roughness (Ra) ranges between (0.1-2.0) µm, is to use a cut-off value (λc) of 0.8 mm with a minimum valuation length of 4mm. This recommendation was followed by setting the sampling length to 0.8mm and five sampling lengths were used to meet the required 4mm for minimum evaluation length. The measurement was repeated three times on each machined surface and their reckoning mean was calculated.

## 3. Results and Discussion

### *3.1 Analysis of Variance for Ra Models*

Lack of fit tests for the suggested model using analysis of variance (ANOVA) is carried out and the results are shown in Table 3 and Table 4 respectively. To improve the quadratic model selected for the $Ra_{PMEDM}$ the insignificant model terms of C, D. AB, AC, BC, and BD in Table 3 were removed from the model. The resulting ANOVA table is shown in Table 4. In the same method, insignificant model terms in the quadratic model for $Ra_{EDM}$ were removed.

**Table 3**
Analysis of variance for $Ra_{PMEDM}$ (reduced model)

| Analysis of variance table [Partial sum of squares - Type III] | | | | | | |
|---|---|---|---|---|---|---|
| Source | Sum of Squares | df | Mean Square | F Value | p-value Prob > F | |
| Model | 157.55 | 3 | 52.52 | 49.55 | < 0.0001 | significant |
| A-Current | 106.47 | 1 | 106.47 | 100.46 | < 0.0001 | |
| B-On-Time | 27.81 | 1 | 27.81 | 26.24 | < 0.0001 | |
| $A^2$ | 23.27 | 1 | 23.27 | 21.95 | < 0.0001 | |
| Residual | 27.56 | 26 | 1.06 | | | |
| Lack of Fit | 23.69 | 21 | 1.13 | 1.46 | 0.3602 | not significant |
| Pure Error | 3.87 | 5 | 0.77 | | | |
| Cor Total | 185.11 | 29 | | | | |

**Table 4**
Analysis of variance for $Ra_{EDM}$ (reduced model)

| Analysis of variance table [Partial sum of squares - Type III] | | | | | | |
|---|---|---|---|---|---|---|
| Source | Sum of Squares | df | Mean Square | F Value | p-value Prob > F | |
| Model | 9.79 | 4 | 2.45 | 17.79 | < 0.0001 | significant |
| A-Current | 1.33 | 1 | 1.33 | 9.70 | 0.0071 | |
| B-On-time | 2.23 | 1 | 2.23 | 16.21 | 0.0011 | |
| $A^2$ | 5.23 | 1 | 5.23 | 38.04 | < 0.0001 | |
| $B^2$ | 1.44 | 1 | 1.44 | 10.46 | 0.0056 | |
| Residual | 2.06 | 15 | 0.14 | | | |
| Lack of Fit | 2.06 | 10 | 0.21 | | 0.1422 | not significant |
| Pure Error | 0.000 | 5 | 0.000 | | | |
| Cor Total | 11.85 | 19 | | | | |

The p-value (Prob>F) column of Table 3 shows p-values of less than 0.05 for the model and model terms A, B, and $A^2$. P-value (Prob>F) column less than 0.05 can equally be observed for model and model terms A, B, and $A^2$ and $B^2$ in Table 4. The p-value of less than 0.05 indicates that both the models and their respective models' terms are significant. The following models were developed for the Ra with and without TaC powder additive EDM.

### *3.2 Developed Model for the Ra*

Eq. (1) and Eq. (2) are the model developed for $Ra_{PMEDM}$ with TaC powder additive and $Ra_{EDM}$ without TaC powder respectively.

The equation developed for $Ra_{PMEDM}$

$$Ra_{PMEDM} = +11.74 + 2.11A + 1.08b\ B - 0.90A^2$$

$$Ra_{PMEDM} = -22.22506 + 5.39891\ Current + 2.69133\ On\text{-}Time - 0.39947\ Current^2 \quad (1)$$

The developed model for $Ra_{EDM}$

$$Ra_{EDM} = +6.44 + 0.31\ A + 0.40\ B - 0.60\ A^2 - 0.31B^2$$

$$Ra_{EDM} = -85.59948 + 2.87285\ Current + 25.76267\ On\text{-}time - 0.26645\ Current^2 - 1.96450\ On\text{-}time^2 \quad (2)$$

It can be seen from Eq. (1) that the most effecting parameters in order of significance are the current and pulse on-time for $Ra_{PMEDM}$. While for $Ra_{EDM}$ on-time is the most effecting parameter followed by current as seen in Eq. (2).

### *3.3 Model Diagnostic Test for Ra*

Validation of the developed models' adequacy is achieved by examining their statistical properties as an extension of the ANOVA table. Lack-of-fit, R-squared, adjusted R-squared, predicted R-squared, and sufficient precision are some of the properties analyzed.

### *3.4 Adequacy of the Developed Ra Model*

An imperfect fit between the data and the model represents the range of values around the fitted model. There will be a serious lack of fit if the model does not adequately represent the data. As seen in Table 3 and Table 4, the discrepancy between the two means that the results are not statistically significant. This demonstrates that Ra's quadratic models provide a good fit for the response data. R-squared is a statistical measure of the proportion of variance in the data that can be attributed to the model. R-squared can be a misleading measure of model quality because it improves when irrelevant terms are included in the model. Adj The R-squared statistic indicates how much of the observed variance the model can account for. If including more terms in the model does not improve the model, the adjusted R-squared will decrease. The amount of new data variation that can be attributed to the model is quantified by its predicted R-squared. The signal-to-noise ratio is the yardstick by which accuracy is evaluated. It evaluates the average prediction error about the spread of predicted values at the design points.

For a model to be measured adequately, the adjusted R-squared value must be greater than 0.7, and the gap between the adjusted and predicted R-squared values must be smaller than 0.2. To ensure adequate model discrimination, a precision ratio of more than 4 is preferred (Design Expert 6.0.8, 2002). Table 5 displays the generated Ra along with its R-squared, adjusted R-squared, predicted R-squared, and adequate precision values.

**Table 5**
Summary Statistic for Ra

| Condition | $Ra_{EDM}$ | $Ra_{PMEDM}$ |
|---|---|---|
| $R^2$ | 0.8259 | 0.8511 |
| Adj $R^2$ | 0.7795 | 0.8340 |
| Pred $R^2$ | 0.7102 | 0.7696 |
| Adeq Precision | 11.979 | 26.846 |

Table 5 shows that one of the requirements for a sufficient model is that the adjusted R-squared (Adj R-Squared) is larger than 0.7. This indicates that for $Ra_{PMEDM}$ (Table 3), 83.40% of the examined variability in Ra can be described by the current and pulse on time. Whereas, for $Ra_{EDM}$ (Table 5), 77.95% of the observed variability in Ra can be explained by current and pulse on time. The adjusted R-squared and predicted R-squared differences are less than 0.2, and the model's adequate precision of 26.846 and 11.979 provide additional evidence of the model's suitability (which is more than 4) and also indicates that the models are adequate.

Model adequacy is usually checked by investigating the errors or residuals from the model. The discrepancies between the actual statements and the fitted values from the regression model are known as errors or residuals. i.e. to check whether residuals are generally dispersed, the normal plot of residuals graph of Figure 5(a) and Figure 5(b) is plotted for $Ra_{PMEDM}$ and $Ra_{EDM}$.

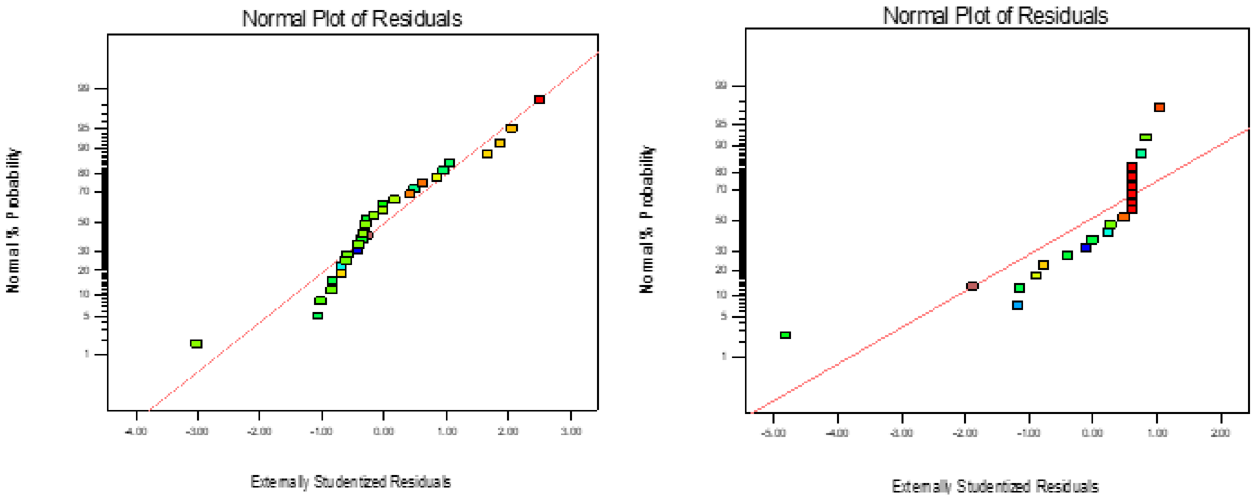

(a) (b)

**Fig. 5.** (a) Normal probability of residuals for $Ra_{PMEDM}$ (b) Normal probability of residuals for $Ra_{EDM}$

The normal prospect plot suggests whether the residuals are distributed normally, in which case a straight line will connect the points. Figure 5(a) and Figure 5(b) also show that the plots are following a straight-line pattern and have a positive value. This confirms that the residuals are generally distributed. The plot of residuals against predicted values will show whether the residual is having the same variance or not. Rizvi *et al.,* [14] pointed out that for a residual plot to represent an ideal situation and to be satisfactory, the plots of residuals versus predicted must have centered around zero, the random distribution of positive and negative values, and finally points should be scattered and there is no obvious pattern.

### *3.5 3-Dimensional Surface and Contour Graphs for $Ra_{PMEDM}$ and $Ra_{EDM}$*

The 3-Dimensional plots and the corresponding contour plots for the models developed for $Ra_{PMEDM}$ are shown in Figure 6. It can be seen (Eq. (1)) that factor current (A) is the major influence on $Ra_{PMEDM}$ followed by factor on-time. The surface plot shows $Ra_{PMEDM}$ 11 μm recorded at current 5A and on-time 6.30 μs, off-time 7.00 μs with powder concentration 25g/L. Also shown in Figure 6 $Ra_{PMEDM}$ is easy to predict by controlling factor current (A) and on-time (B). At the higher current of 7.25A, $Ra_{PMEDM}$ showed to decrease slightly. This result justifies TaC powder starts to control and modify the surface of stainless steel at a high factor current (A).

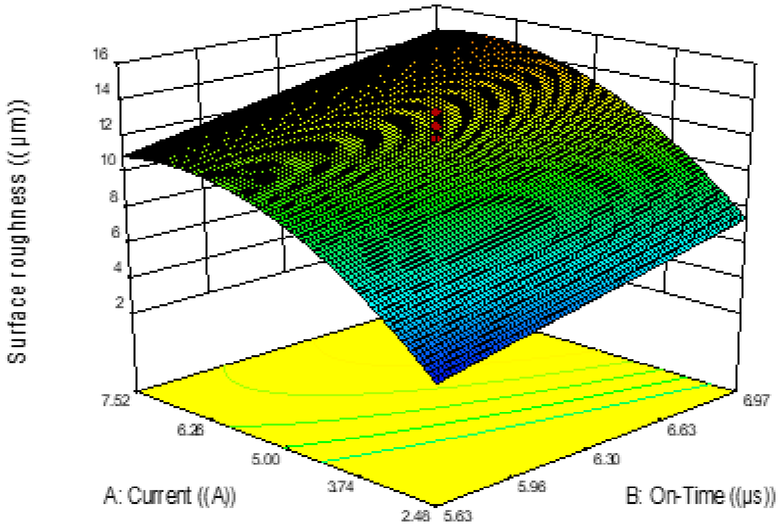


**Fig. 6.** 3-D surface plots of $Ra_{PMEDM}$ with current and on time

The 3-Dimensional surface and contour plots for the surface roughness without TaC powder additive, $Ra_{EDM}$ is shown in Figure 7. It can be observed (Eq. (2)) for the $Ra_{EDM}$ model that there is an interaction between factor current and pulse on time. Figure 7 also shows that by increased factors current and on-time $Ra_{EDM}$ will increase in a quadratic pattern where at maximum current 5 A, on-time 6.26 μs, and off-time 7 μs, $Ra_{EDM}$ recorded 7 μm. Although it provided the highest Ra compare to $Ra_{PMEDM}$ it had limited function during the highest current machining.

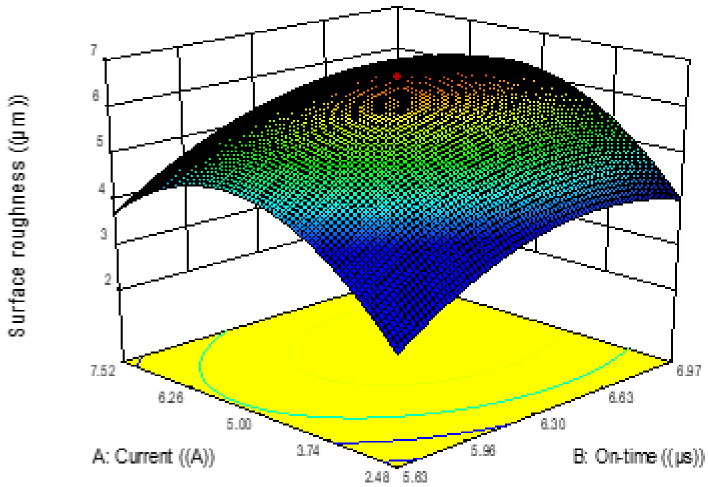


**Fig. 7.** 3-D surface plots of $Ra_{EDM}$ with current and on time

### *3.6 Model Predictability for Ra*

The next graph to be plotted in the analysis of the model established for Ra is the checking of the predicted (calculated) against actual (measured) response values. The plot is expected to be scattered along a straight line. Figure 8(a) and Figure 8(b) shows the scattered plot between the predicted and actual values of the response for Ra confirming the model adequacy within the experimental region. Those figures show the discrepancies in the actual and predicted values of $Ra_{PMEDM}$ and $Ra_{EDM}$ respectively. The plots demonstrate less variation between the two sets of data, demonstrating the model's ability to predict response.

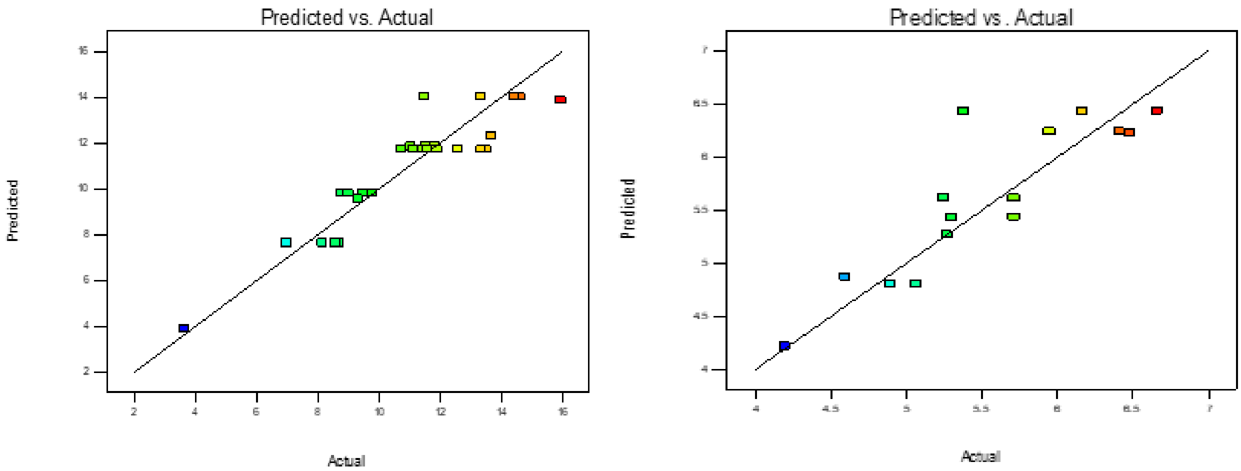


(a) (b)

**Fig. 8.** (a) Scattered plots of predicted against the measured values for $Ra_{PMEDM}$, (b) Scattered plots of predicted against the measured values for $Ra_{EDM}$

## 4. Conclusions

This study aimed to evaluate the efficiency of EDM-based surface alloying of stainless steel using Tantalum Carbide (TaC) powder as an additive by measuring the resulting surfaces' roughness (SR). It was found that $Ra_{PMEDM}$ 11 µm recorded at current 5A and on-time 6.30 µs, off-time 7.00 µs with powder concentration 25g/L. The $Ra_{PMEDM}$ is easy to predict by controlling factor current (A) and on-time (B). At the higher current of 7.25A, $Ra_{PMEDM}$ showed to decrease slightly. This result justifies that TaC powder starts to control and modify the surface of stainless steel at a high factor current. In the case of without additives $Ra_{EDM}$, at maximum current 5 A, on-time 6.26 µs, and off-time 7 µs, $Ra_{EDM}$ recorded 7 µm. Although it provided the highest Ra compared to $Ra_{PMEDM}$.

## Acknowledgment

The International Islamic University Malaysia's machining lab, workshop, and SEM lab were used for the research. The author is appreciative of the contemporary lab setting as well as the lab assistant's assistance.

## References

[1] Rashid, Mir Akmam Noor, Tanveer Saleh, Wazed Ibne Noor, and Mohamed Sultan Mohamed Ali. "Effect of laser parameters on sequential laser beam micromachining and micro electro-discharge machining." *The International Journal of Advanced Manufacturing Technology* 114 (2021): 709-723. https://doi.org/10.1007/s00170-021-06908-8

[2] Gopalakannan, Subramanian, and Thiagarajan Senthilvelan. "Optimization of machining parameters for EDM operations based on central composite design and desirability approach." *Journal of Mechanical Science and Technology* 28, no. 3 (2014): 1045-1053. https://doi.org/10.1007/s12206-013-1180-x

[3] Shinde, Rajendra, Nilesh Patil, D. Raut, Raju Pawade, and Prakash Brahmaknakr. "Experimental investigations into powder-mixed electrical discharge machining (PMEDM) of HCHCR D2 die steel." In *International Conference on Communication and Signal Processing 2016 (ICCASP 2016)*, pp. 298-303. Atlantis Press, 2016. https://doi.org/10.2991/iccasp-16.2017.47

[4] Bhaumik, Munmun, and Kalipada Maity. "Effect of machining parameter on the surface roughness of AISI 304 in silicon carbide powder mixed EDM." *Decision Science Letters* 6, no. 3 (2017): 261-268. https://doi.org/10.5267/j.dsl.2016.12.004

[5] Ibne, Noor Wazed, Saleh Tanveer, Rashid Mir Akmam Noor, Mohd Ibrahim Azhar, and Ali Mohamed Sultan Mohamed. "Dual-stage artificial neural network (ANN) model for sequential LBMM-μEDM-based micro-drilling." *The International Journal of Advanced Manufacturing Technology* 117, no. 11-12 (2021): 3343-3365. https://doi.org/10.1007/s00170-021-07910-w

[6] Chiang, Ko-Ta. "Modeling and analysis of the effects of machining parameters on the performance characteristics in the EDM process of $Al_2O_3$+ TiC mixed ceramic." *The International Journal of Advanced Manufacturing Technology* 37, no. 5-6 (2008): 523-533. https://doi.org/10.1007/s00170-007-1002-3

[7] Goyal, Shivam, and Rakesh Kumar Singh. "Parametric study of powder mixed EDM and optimization of MRR & surface roughness." *International Journal of Scientific Engineering and Technology* 3, no. 1 (2014): 56-62.

[8] Ojha, Kuldeep, R. K. Garg, and K. K. Singh. "Experimental investigation and modeling of PMEDM process with chromium powder suspended dielectric." *International Journal of Applied Science and Engineering* 9, no. 2 (2011): 65-81.

[9] Abbas, Norliana Mohd, Darius G. Solomon, and Md Fuad Bahari. "A review on current research trends in electrical discharge machining (EDM)." *International Journal of Machine Tools and Manufacture* 47, no. 7-8 (2007): 1214-1228. https://doi.org/10.1016/j.ijmachtools.2006.08.026

[10] Chakraborty, S., V. Dey, and S. K. Ghosh. "A review on the use of dielectric fluids and their effects in electrical discharge machining characteristics." *Precision Engineering* 40 (2015): 1-6. https://doi.org/10.1016/j.precisioneng.2014.11.003

[11] Uhlmann, Eckart, and Markus Roehner. "Investigations on reduction of tool electrode wear in micro-EDM using novel electrode materials." *CIRP Journal of Manufacturing Science and Technology* 1, no. 2 (2008): 92-96. https://doi.org/10.1016/j.cirpj.2008.09.011

[12] Lee, Hwa Teng, and Tzu Yao Tai. "Relationship between EDM parameters and surface crack formation." *Journal of Materials Processing Technology* 142, no. 3 (2003): 676-683. https://doi.org/10.1016/S0924-0136(03)00688-5

[13] Selvarajan, L., R. Rajavel, K. Venkataramanan, T. Elango, and M. Dhinagaran. "An experimental investigations and optimization of performance measures in EDM using copper and graphite electrodes." *Materials Today: Proceedings* 46 (2021): 9341-9347. https://doi.org/10.1016/j.matpr.2020.02.816

[14] Rizvi, Syed Asghar Husain, Sanjay Agarwal, and Prem K. Bharti. "Modeling of Surface Roughness of AISI 4340 Using Copper-Tungsten Tool in Die Sinking EDM." *Materials Today: Proceedings* 22 (2020): 2334-2340. https://doi.org/10.1016/j.matpr.2020.03.355

[15] Mahmud, Nazriah, and Azli Yahya. "Consistent Machining of Electrical Discharge Machining Power Supply Towards Hip Implant Surface Texturing." *Journal of Advanced Research in Applied Sciences and Engineering Technology* 11, no. 1 (2018): 39-46.

[16] Ali, M. A. Md, S. Laily, B. Manshoor, N. I. Syahrian, R. Izamshah, M. Hadzley, and M. R. Muhamad. "Performance of copper, copper tungsten, graphite and brass electrode on MRR, EWR and SR of aluminium LM6 in EDM die sinking." *Journal of Advanced Research in Applied Mechanics* 6, no. 1 (2015): 30-36.